

## Molecular Dynamics Simulation on Formation of Ge Thin Film for Flexible Communication Devices

\* **Yoshiaki KOGURE, Tomoko FUNAYAMA and Yasutaka UCHIDA**

Teikyo University of Science  
Adachi-ku, Tokyo, Japan  
Tel.: + 81-47-411-6265  
\* E-mail: kogure@ntu.ac.jp

*Received: 30 August 2019 / Accepted: 27 September 2019 / Published: 30 November 2019*

---

**Abstract:** Materials for flexible sensor that operate in close contact with the skin has been investigated. The sensor maintain the quality of life and the communication device for disabled people. Low-temperature crystallization and mechanical properties of Germanium thin films have been simulated by means of molecular dynamics under free boundary condition. Tersoff bond order potential was adopted for calculating the interactions between germanium atoms. Amorphous model was prepared by quenching the molten system at 1800 K. The model was consisted of 10,500 atoms. By annealing the amorphous state at 400 K, partial crystallization was realized. Crystallization was verified by the radial distribution function of the model. Then the film was deformed and stress-strain relation was calculated. The change of atomic structure during the deformation was investigated from the cross-sectional views. The mechanical strength and flexibility are discussed from microscopic point of view. Simulation plays a complementally role with the experimental research and contributes to the development of the flexible sensors.

**Keywords:** Germanium thin film, Molecular dynamics, Tersoff potential, Crystallization, Stress-strain relation, Flexible sensor, Communication device.

---

### 1. Introduction

A flexible sensor that functions closely to the skin is an indispensable tool in the field of care and rehabilitation. Recently, it has become possible to measure the vital signs for a long time. In order to be able to measure in daily life, it is necessary to have a flexible sensor that can be deformed according to the shape of skin. Resetting is required when a gap appears between sensor and skin. Stable sensor operation is really required. We have been studying hemoglobin measurement as a communication device for disabled people. Such a device employs near-infrared spectroscopy (NIRS) [1]. The fabrication of sensors that adhere to the skin is essential to accurately

measure the oxyhemoglobin in the blood flow. The present authors have been engaged in the study to fabricate the germanium thin films on the flexible substrates in the project to improve the yes/no device [2-3]. The low-temperature metal-induced polycrystallization of electrodeposited germanium thin film on flexible substrate has been realized experimentally. Germanium has a high carrier mobility and low processing temperature. In our experimental study germanium films are deposited at 60°C and crystallized at 150°C (423 K). However, the microscopic process of the mechanism of crystallization is not well understood in many cases [4-5]. Molecular dynamics simulation is a powerful way to visualize microscopic processes of

crystallization [6-7]. One of the present authors has been applied the molecular dynamics simulation on the studies of crystal defects and mechanical properties of metals [8]. The program code developed in the studies can be utilized in the present investigation.

## 2. Method of Simulation

### 2.1. Atomic Potential

The bond order potential function developed by Tersoff is used in the simulation [9-10]. The potential energy depends on the bond length and bond angle. The potential energy is described as

$$E = \sum_i E_i, \quad E_i = \frac{1}{2} \sum_{j \neq i} V_{i,j}, \quad (1)$$

$$V_{ij}(r) = f_C(r)[f_R(r) + b_{ij}f_A(r)], \quad (2)$$

$$\begin{aligned} f_R &= A \exp(-\lambda r), \\ f_A &= -B \exp(-\mu r), \end{aligned} \quad (3)$$

where  $f_C(r)$  is the truncation function,  $b_{ij}$  is related to the coordination number and represent the many body nature of the potential. Constants  $A, B, \lambda, \mu$  are determined to reproduce the experimental values of physical property. The elementary structure of germanium is shown in Fig. 1 (A). The potential energy depends on the bond length  $r$  and the bond angle  $\theta$ . The contour plot for the potential energy of central atom is shown in Fig. 2. The energy shows a minimum at  $r = 2.43$  angstrom and  $\theta = 116$  deg. The force acting on an atom is calculated by differentiating the energy by distance  $r$ .

### 2.2. Molecular Dynamics

The equation of motion for an atom is solved by integrating the potential numerically by the Verlet algorithm. The time interval for the numerical integration is chosen to be  $\Delta t = 1.0 \times 10^{-15}$  sec, which is much smaller than the period of the thermal vibration in germanium.

The temperature of the atomic system can be controlled by rescaling the mean velocity  $\langle v^2 \rangle$  of atoms through the relation  $m \langle v^2 \rangle = 3kT$ , where  $m$  is the atomic mass and  $k$  is the Boltzmann constant. The simulations are performed by using a FORTRAN code developed by the present authors and results are visualized by Visual Basic (Microsoft).

As a simplest simulation, snapshots in free vibration of three atomic system in shown in Fig. 1. Contour plot of the potential energy for central atom is

shown in Fig. 2. White circles indicated by A, B and C in the figure are corresponding to the arrangement shown in Fig. 1.

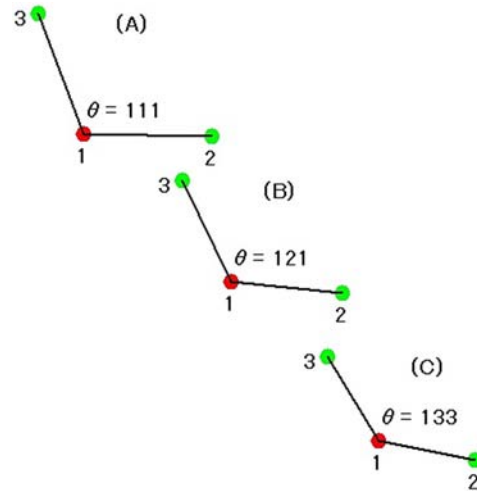


Fig. 1. Configuration of atoms in elementary structure under free oscillation.

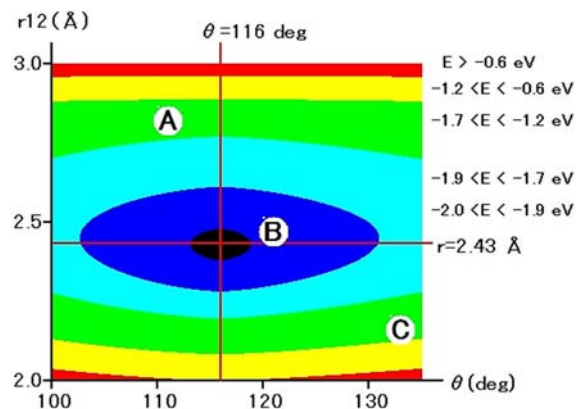
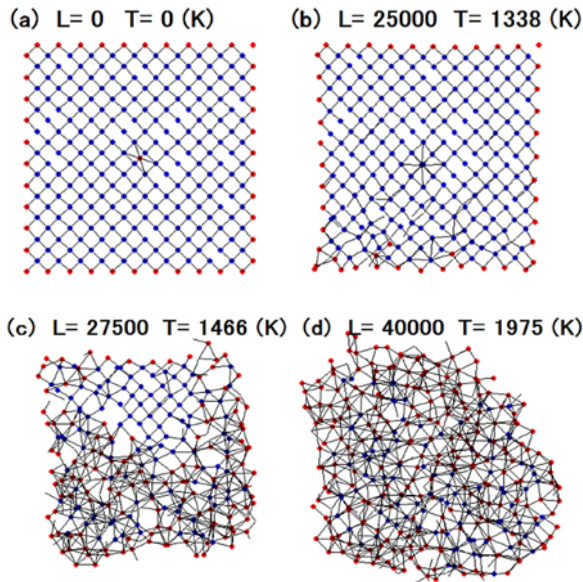


Fig. 2. Contour plot of potential energy of Tersoff potential for the central atom in the elementary structure.

## 3. Results and Discussion

### 3.1. Simulation in Small Cubic Sample

In order to set the parameters for simulation, the calculation was initially performed on a relatively small cubic sample of a diamond structure with {100} surfaces. The sample was consisted of about 1000 atoms and free boundary condition was adopted for the simulation. The crosssectional view of atomic configuration in the initial state is shown in Fig. 3(a). Where  $L$  show the molecular dynamics time step (MD step). When the temperature of the sample is raised by increasing the mean velocity at a certain rate, the structural disorder starts around the bottom. The disorder may proceed from the periphery to the inside as the temperature rises as shown in Figs. (b), (c) and (d). Eventually the whole sample is in a molten state at around 2000 K.



**Fig. 3.** Configuration of atoms in cubic sample during heating.

Four atoms in the vicinity of the center were selected as sample atoms. Trajectories of those atoms during the temperature rise are shown in Fig. 4 (a). The zigzag trajectory appears to be due to the diffusion of atoms in the molten state. Fig. 4 (b) shows the temperature change with respect to the simulation step (time). It can be seen that the temperature rises to around 2000 K at a constant rate and then controlled to be constant. The displacements from the starting points of sample atoms are plotted against the time step in Fig. 4 (c). The colour coding of sample atom is the same as Fig. (a). In the first half of the simulation, the sample atoms are hardly moving, but when they reach a certain temperature, they start moving all at once. Its temperature is 1250 K, close to the melting temperature of Ge. That is, it can be seen that not only static structure but also the sample is melted dynamically.

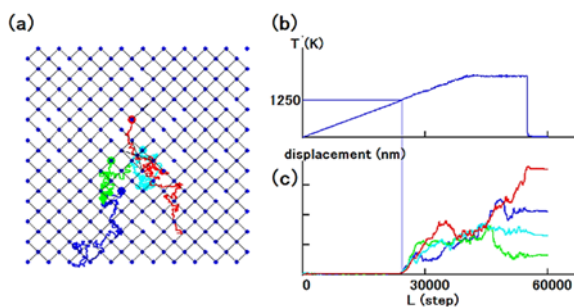


**Fig. 4.** Trajectory and displacement of sample atoms during heating (a), time variation of sample temperature (b), and displacements from initial positions.

Fig. 5 shows histograms of the velocity distributions of atoms in the specimen being heated. As is well known, the velocity in thermal equilibrium follows the Maxwell distribution

$$f(v) = 4\pi v^2 \left( \frac{m}{2\pi kT} \right)^{3/2} \exp\left( -\frac{mv^2}{2kT} \right) \quad (4)$$

The solid lines in the figure show the calculated Maxwell distribution for each temperature. In the simulation, the initial velocity given to the atoms is generated by a uniform random number. As the simulation proceeds, it can be seen that the velocity distribution approaches the Maxwell distribution.

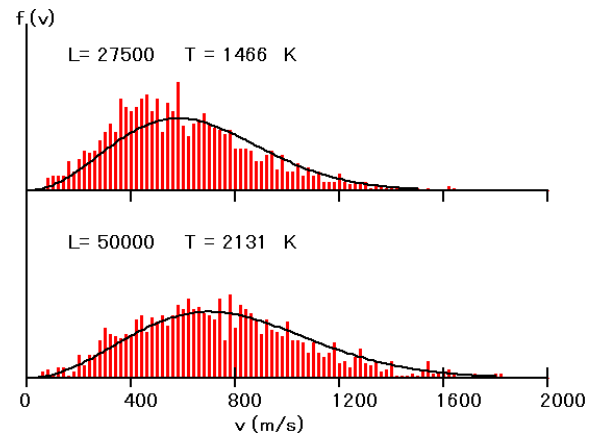


**Fig. 5.** Velocity distribution of atoms at elevated temperatures.

### 3.2. Crystallization of Cubic Sample

When a sample in a molten state is rapidly cooled, an amorphous state appears. This is a state where a disordered atomic arrangement in a liquid state is frozen. Fig. 6(a) shows an amorphous state produced by quenching the molten state shown in Fig. 3(d). The radial distribution function is shown on the right side. A sharp peak is observed around 2,5 angstrom, followed by irregular fluctuations.

It is known that atomic configuration in an amorphous state is unstable and crystallizes at a relatively low temperature. Fig. 6(b) and (c) show the process of crystallization at around 400 K. In Fig. 6(b), it can be seen that crystallization has started in the area indicated by A and B. Furthermore, when the simulation is continued at that temperature, crystallization progresses, and it can be seen that the whole sample approaches one single crystal. The external shape of the sample shows a crystal shape surrounded by linear planes, and the radial distribution function has a pulse shape, which is also characteristic of crystal.

### 3.3. Formation of Thin Film Sample

Thin film samples for the simulation is consisted of 10,500 atoms. In the initial state, atoms are arranged in a perfect crystal of diamond structure of rectangular shape with {100} faces. The size is 9 nm×9 nm×3 nm, as shown in Fig. 7(a), where the nearest neighbor atoms are connected by straight lines.

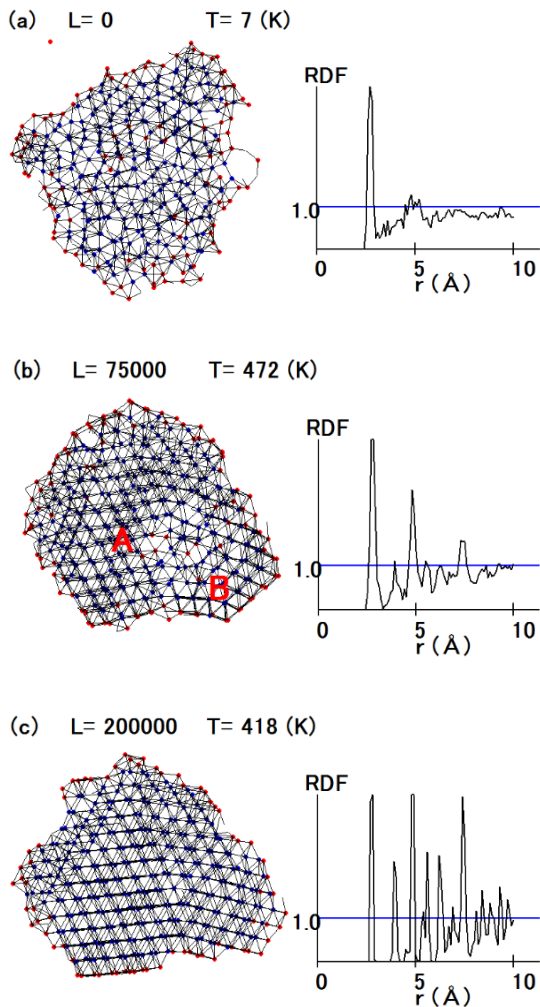


Fig. 6. Crystallization of cubic sample from amorphous state.

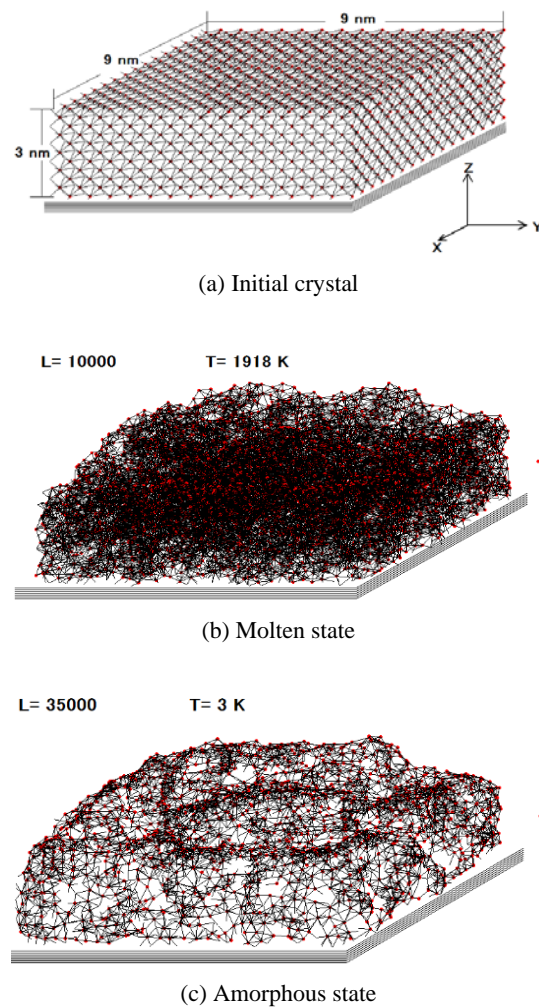


Fig. 7. Preparation of amorphous sample.

Then the temperature is raised to 1900 K or more to bring it into a molten state (Fig. 7(b)). The atoms in the system of molten state are in completely disordered state. After keeping in the molten state for 30,000 MD steps the system is suddenly quenched to 0 K, and then the amorphous state is realized as shown in Fig. 7(c). The temperature variation during the amorphization process is shown as a function of MD step in Fig. 8. The temperature in molten state is seen to be controlled flat and suddenly drops to 0 K.

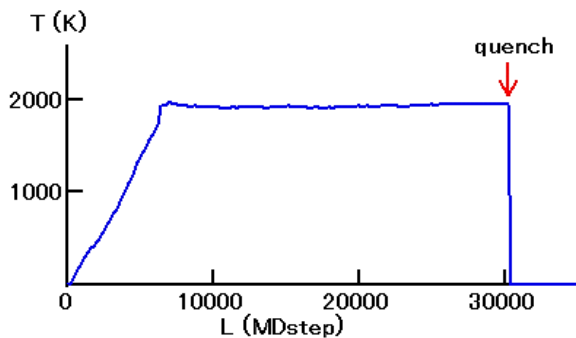


Fig. 8. Temperature variation during amorphization.

### 3.4. Crystallization of Thin Film at 400 K

In the experimental study, Cu-induced polycrystallization of electrodeposited films were observed at 150 °C (423 K). The molecular dynamics simulations for annealing and crystallization in large thin film (10,500 atoms) samples were performed at 400 K, where the metal element was not involved. Two types of boundary conditions between the sample and the substrate were tried.

1) The substrate and the sample are in closely contacted and atoms can slide on the surface.

2) The sample is loosely contacted with the substrate allowing a gap within 10 angstrom.

In the boundary condition 1), crystallization has hardly progressed because atoms are mostly fixed at the lower end. On the contrary, in the boundary, condition 2), it can be seen that polycrystallization is more advanced because of the boundary close to the free surface even at the lower end. An example of crystallization at the substrate is shown in Fig. 9. A progress of crystallization at the left side is seen. In order to occur a crystallization, a degree of freedom in the three-dimensional direction may be necessary at

the surface. Namely, the boundary condition is very important for the crystallization of thin films.

Atomic structure in a plane parallel to the bottom of thin film is shown in Fig. 11. It is a heterogeneous structure of crystalline and amorphous parts. The radial distribution function (RDF) at typical zones (A), (B), (C) are inserted in the figure. RDF in regions (A) and (B) show crystalline character, but RDF in (B) is sharper and has shown higher crystallinity than (A). RDF in (C) shows disordered and amorphous nature.

Judging from Fig. 9 and Fig. 11, the characteristic sizes of the crystalline and amorphous regions appear to be comparable to the thickness of thin film. Typical time steps of the molecular dynamics is 100,000.

Meanwhile the outershape and the heterogeneous structure of films were changing. The average potential energy of atoms increased once, and decreased again. At that time, a change in heterogeneous structure was observed. Simulation at a different temperature, 500 K, was performed, and similar behavior was seen. The movement of atoms was more intense when the temperature was higher.

Fig. 10 show the change in potential energy of small cubic sample and large thin film sample during the crystallization processes. In the cubic sample, energy decreases monotonically and crystallization progresses, whereas in the thin film sample, energy decreases slowly while increasing and decreasing repeatedly. In the thin film sample, crystallization begins in each part, and it seems that the growth of grain boundaries with different orientations pushing each other. The smaller cubic sample has higher potential energy per atom because the proportion of atoms present on the sample surface is large.

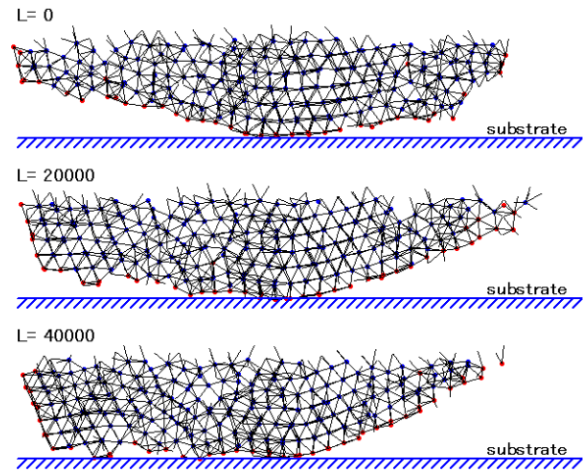


Fig. 9. Crystallization near substrate under loosely contacted boundary condition.

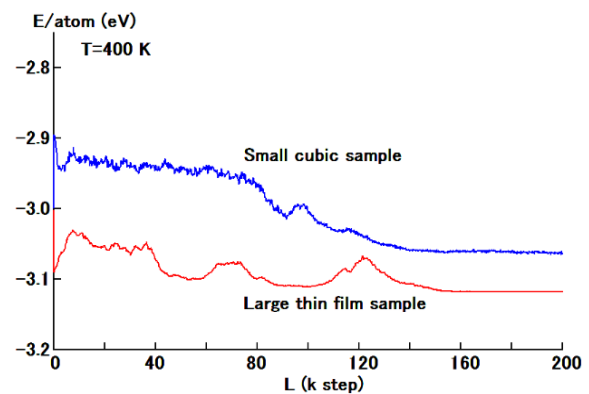


Fig. 10. Change of potential energy in cubic and thin film samples.

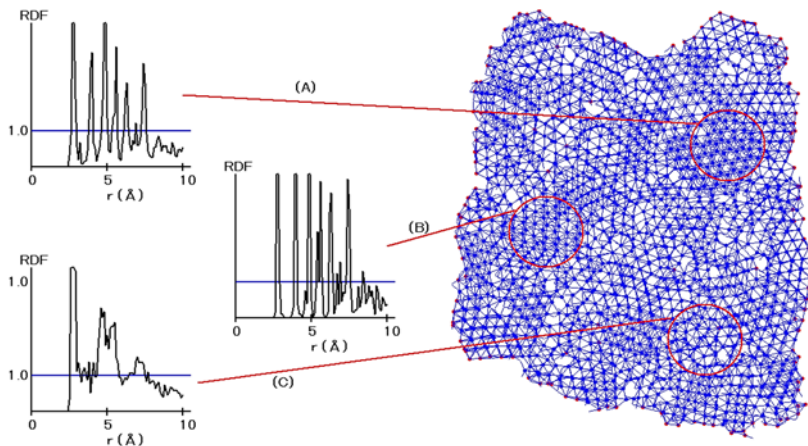
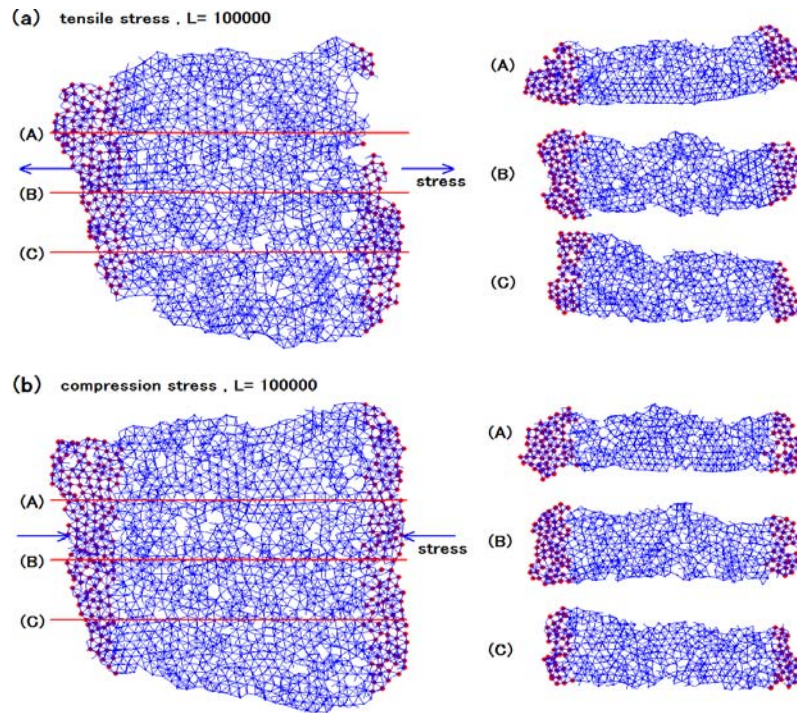


Fig. 11. Annealed thin film sample and radial distribution functions.

### 3.5. Mechanical Properties

Tensile and compression stresses were applied on the thin film sample. The atomic configuration during deformation is shown in Fig. 12, where the atoms shown by red circles are rigidly displaced in opposite directions to apply the tensile and compression strains. The strain rate is  $1.6 \times 10^9$  /sec and maximum strain

is about 8%. The stress can be calculated from the sum of the forces acting on fixed atoms during deformation. In fact, since the forces acting on atoms inside the fixed region cancel each other. Only the forces at the boundary remain and contribute to the stress. Calculated stress-strain relation is shown in Fig. 13.



**Fig. 12.** Atomic structure in tensile (a) and compression (b) deformation. Shown on the right of each figure are the atomic arrangements of the cross-section cut along the A, B and C planes.

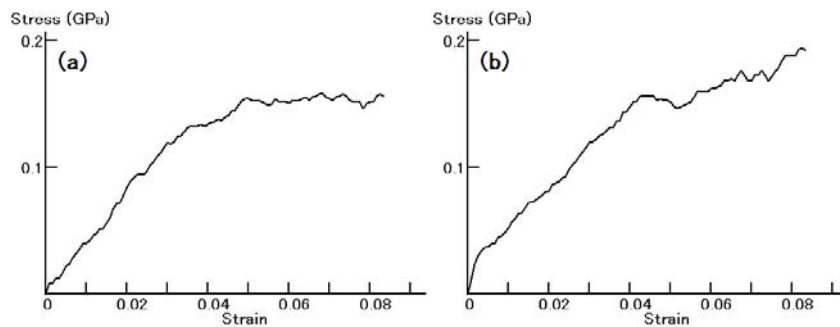


**Fig. 13.** Stress-strain relations in tensile (a) and compression (b) deformation.

The stress is seen to be increasing in proportion to the strain in the first part of the stress-strain relation in Fig. 13. Young's modulus may be able to be estimated as 3 GPa, which is much smaller than the perfect crystal of germanium. This may be due to the sparse structure of present sample. The stress approaches a constant value at a strain of 4 % or more. The atomic structure during deformation is a mixture of crystalline parts and amorphous disordered structures as shown in Fig. 12. The mosaic structure changes as the deformation progressed. The mechanism of deformation of this thin film seems to be similar to the deformation of polycrystals by slippage of grain boundaries. The motion of dislocations and other point defects might be concerned.

#### 4. Possibility for Flexible Devices

In recent years, interest in bending and expanding material has increased in the healthcare field for vital

sensing. In general, a flexible material such as a polymer has no heat resistance, and it is desirable that an amorphous semiconductor deposited thereon is crystallized at a relatively low temperature. Ge that crystallizes at about 400 K (130 °C) is a suitable material. Recently, the appearance of 1 – 2 nm clusters during Ge crystallization was discovered by a transmission electron microscope and attracting attention. The present study seems to be effective in elucidating the micro process.

#### 5. Conclusions

Low temperature crystallization of germanium thin film has been simulated by means of molecular dynamics using Tersoff potential. In particular, the movement of individual atoms at the interface with the substrate was found to be important. This point is really helpful in the experimental study. The

heterogeneous structure consist of crystalline and amorphous regions was realized. Basic calculation on the mechanical properties of germanium thin films were also made. The stress-strain relation of heterogineeous film was successfully delivered by the simulation. The analysis of flexible natures of sensors linked to actual skin movement is difficult because the models that can be handled by molecular dynamics are too small. Adoption of multiscale model combining atomic model with continuum model seems to be effective.

Present study explore the communication possibility of disabled people. The accuracy of measurement indoor life has increased. However it may not be used outdoors with heavy activity, because the device still lacks flexibility and stability.

## References

- [1]. M. Naito, Y. Michioka, K. Ozawa, I. Ito, M. Kiguchi, T. Kanazawa, A communication means for totally locked-in ALS patients based on changes in cerebral blood volume measured with near-infrared light, *IEICE Transactions on Information and Systems*, Vol. E90-D, Issue 7, 2007, pp. 1028-1037.
- [2]. Y. Uchida, T. Funayama, Y. Kogure, W. Yeh, Metal-induced low-temperature crystallization of electrodeposited Ge yjin film, *Japanese Journal of Applied Physics*, Vol. 55, Issue 3, 2016, pp. 031303-1–031303-5.
- [3]. Y. Uchida, T. Funayama, Y. Kogure, W. Yeh, Low-temperature Cu-induced poly-crystallization of electrodeposited germanium thin film on flexible substrate, *Physica Status Solodi C*, Vol. 13, Issue 10-12, 2016, pp. 864-867.
- [4]. D. Shahrjerdi, B. Hekmatshoar, S. S. Mohajerzadeh, A. Khakifirooz, M. Robertson, High Mobility Poly-Ge Thin-Film Transistors Fabricated on Flexible Plastic Substrates at Temperatures below 130° C, *Journal of Electronic Materials*, Vol. 33, Issue 4, 2004, pp. 353-357.
- [5]. W. Knaepen, S. S. Gaudet, C. Detavernir, R. L. Van Meirhaeghe, J. Jordan Sweet, C. Lavoie, In situ x-ray diffraction study of metal induced crystallization of amorphous germanium, *Journal of Applied Physics*, Vol. 105, Issue 8, 2009, pp. 083532-1–083532-7.
- [6]. Y. Kogure, T. Funayama, Y. Uchida, Atomistic Simulation of Structure and Dynamics in Crystallizing Germanium Thin Films, *Sensors & Transducers*, Vol. 227, Issue 11, November 2018, pp. 21-27.
- [7]. Y. Kogure, T. Funayama, Y. Uchida, Simulation of Crystallization and Mechanical Properties of Ge Thin Film for Flexible sensor in Communication Devices, in *Proceedings of the 5<sup>th</sup> International Conference on Sensors and Electronic Instrumentation Advances (SEIA' 2019)*, Tenerife (Canary Islands), Spain, 25-27 September 2019, pp. 88-91.
- [8]. Y. Kogure, Y. Hiki, Atomistic Simulation of Shear Mode Deformation of Nanocrystalline Copper with Different Grain Sizes, *Materials Transactions*, Vol. 55, Issue 1, 2014, pp. 64-68.
- [9]. J. Tersoff, New empirical approach for the structure and energy of covalent systems, *Physical Review B*, Vol. 37, Issue 12, 1988, pp. 6991-7000.
- [10]. J. Tersoff, Modeling solid-state chemistry: interatomic potential for multicomponent systems, *Physical Review B*, Vol. 39, Issue 8, 1989, pp. 5566-5568.



Published by International Frequency Sensor Association (IFSA) Publishing, S. L., 2019  
(<http://www.sensorsportal.com>).



**Sensors Industry  
News**

**FREE Monthly  
IFSA Newsletter**

ISSN 1726-6017

**SUBSCRIBE NOW**  
[subscribe@sensorsportal.com](mailto:subscribe@sensorsportal.com)